PHYSICAL REVIEW B **92**, 060403(R) (2015)

Giant forward-scattering asymmetry and anomalous tunnel Hall effect at spin-orbit-split and exchange-split interfaces

T. Huong Dang,[1] H. Jaffrès,[2] T. L. Hoai Nguyen,[3] and H.-J. Drouhin[1,*]
[1]*Laboratoire des Solides Irradiés, Ecole Polytechnique, CNRS UMR 7642, and CEA-DSM-IRAMIS, Université Paris-Saclay, 91128 Palaiseau cedex, France*
[2]*Unité Mixte de Physique CNRS-Thales, 1, Avenue Augustin Fresnel, 91767 Palaiseau and Université Paris-Sud, 91405 Orsay, France*
[3]*Institute of Physics, VAST, 10 Daotan, Badinh, Hanoi, Vietnam*

(Received 16 March 2015; revised manuscript received 15 May 2015; published 5 August 2015)

We report on theoretical investigations of scattering asymmetry vs incidence of carriers through exchange barriers and magnetic tunnel junctions made of semiconductors involving spin-orbit interaction. By an analytical 2×2 spin model, we show that when Dresselhaus interaction is included in the conduction band of antiparallel magnetized electrodes, the electrons can undergo a large difference of transmission depending on the sign of their incident in-plane wave vector. In particular, the transmission is fully quenched at some points of the Brillouin zone for specific in-plane wave vectors and not for the opposite. Moreover, the asymmetry is universally scaled by a unique function independent of the spin-orbit strength. This particular feature is reproduced by a 14×14 band $\mathbf{k} \cdot \mathbf{p}$ model showing, in addition, corresponding effects in the valence band and highlighting the robustness of the phenomenon, which even persists for a single magnetic electrode. Upon tunneling, electrons undergo an asymmetrical deflection which results in the occurrence of a transverse current, giving rise to a so-called tunnel Hall effect.

DOI: 10.1103/PhysRevB.92.060403 PACS number(s): 72.25.Mk, 75.70.Tj, 75.76.+j

The interplay between particle spin and orbital motion is currently the basis of new functionalities. These require efficient spin-current injection at magnetic-nonmagnetic interfaces, efficient spin-transfer torque, and possibly efficient spin Hall effect with heavy materials [1–4] for magnetic commutation. Spin-orbit interaction (SOI) at an interface with broken inversion symmetry may lead to the observation of Rashba-split states [5–8] which can be used to convert a perpendicular spin current into a lateral charge current by inverse Edelstein effect (IEE) [9,10]. In that context, investigations of SOI in solids and at interfaces is of prime importance for basic physics and today's technology.

In this Rapid Communication, we study unconventional quantum effects resulting in giant transport asymmetry for electrons or holes in structures composed of exchange and spin-orbit-split electrodes made of III-V semiconductors with antiparallel (AP) magnetizations, possibly separated by thin tunnel barriers. The symmetry of the structure allows a transmission difference vs carrier incidence near interfaces with respect to the reflection plane defined by the magnetization and the surface normal. This quantum process departs from the effect of a beam deviation by the Lorentz force due to the action of a local magnetic field in the barrier [11] and from spin-filtering effects occurring in noncentrosymmetric structures [12,13]. Unlike the latter, the effect we propose requires the simultaneous action of both in-plane and out-of plane spin-orbit fields for promoting transport spin asymmetry. In order to address the issue in a simple way, we first consider a heterojunction made of two identical magnetic semiconductors of zinc-blende symmetry, with opposite in-plane magnetizations: this structure (Fig. 1) constitutes an ideal exchange step and is a paradigm for exchange-engineered heterostructures, similarly to symmetrical spin valves in giant magnetoresistance [14,15]. Indeed, due to the axial character of the magnetization, the AP configuration breaks the symmetry with respect to the reflection plane (in Fig. 1 the reflection plane is the xz plane), and also some possible rotation and time conjugation invariances existing in the parallel (PA) magnetic arrangement [16]. The result is that two waves with opposite in-plane wave vectors $\mathbf{k}_{\parallel}$ may be differently transmitted in amplitude.

We first consider SOI in the conduction band of bulk materials through the Dresselhaus contribution [17]. Hereafter, we refer the structure to the x,y,z cubic axes (unit vectors $\widehat{x},\widehat{y},\widehat{z}$) and assume that electron transport occurs along the z axis, whereas the magnetization lies along x. We study the transmission asymmetry when the wave vector component along y is changed from ξ to $-\xi$. Electrons are injected from the first conduction band of material I to the left ($\epsilon = 1$) into the first conduction band of material II to the right ($\epsilon = -1$). Then, the relevant 2×2 Hamiltonians are respectively written

$$\widehat{H}_{I,II} = \gamma_c(k^2+\xi^2)\widehat{I} + w\mathbf{m}\cdot\widehat{\sigma} + (\widehat{\gamma}\chi)\cdot\widehat{\sigma} = \begin{pmatrix} \gamma_c(k^2+\xi^2) - \widetilde{\gamma}\xi^2 k & -i\gamma\xi k^2 + \epsilon w \\ i\gamma\xi k^2 + \epsilon w & \gamma_c(k^2+\xi^2) + \widetilde{\gamma}\xi^2 k \end{pmatrix}, \quad (1)$$

where $(0,\xi,k)$ is the electron wave vector; $\widehat{I}$ is the identity matrix, γ_c accounts for the conduction effective mass, $\mathbf{m}$ is the unit magnetization vector, $2w$ the exchange splitting (assumed to be positive), $\widehat{\sigma}$ the Pauli operator, and $\chi = [0,\xi k^2,-\xi^2 k]$ the D'yakonov-Perel' (DP) internal field responsible for the spin splitting [17,18]. For the subsequent discussion, we introduce the tensor $\widehat{\gamma} = (\gamma_i \delta_{ij})$ which characterizes the DP-field strength, with $\gamma_x = \gamma_y = \gamma$, $\gamma_z = \widetilde{\gamma}$, and δ_{ij} the Kronecker symbol. We consider the two cases $\widetilde{\gamma} = \gamma$ and $\widetilde{\gamma} = 0$, switching on and off the ξ^2 diagonal perturbation.

The two energies in the exchange and spin-orbit-split subbands are given by $\mathcal{E}_1 = \gamma_c(k_1^2+\xi^2) - w$ and $\mathcal{E}_2 =$

*Corresponding author: henri-jean.drouhin@polytechnique.edu

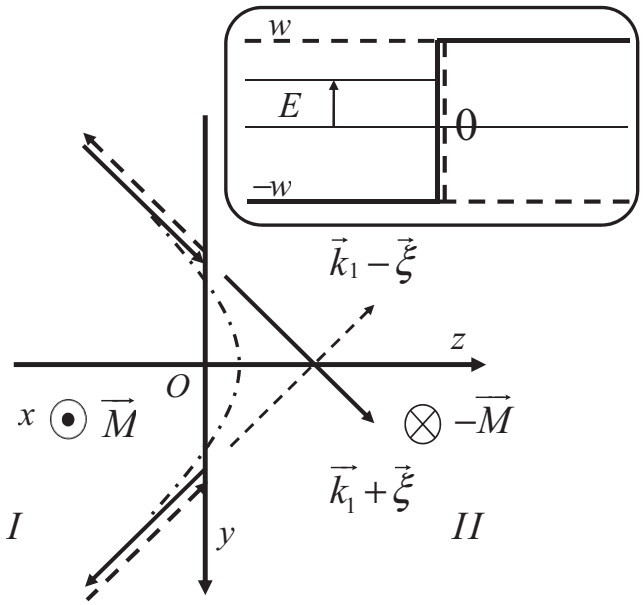

FIG. 1. Scheme of transmission process at an exchange-SOI step with AP magnetizations **M** and $-\mathbf{M}$ along x. The propagation direction of carriers (straight arrow) is along z with propagative wave vector k_1 whereas the in-plane incident component $+\xi$ (heavy line) or $-\xi$ (dashed line) is along y; **xyz** forms a direct frame. The dash-dotted curve denotes the evanescent waves, either reflected or transmitted. Carriers with $+\xi$ in-plane wave vector component are more easily transmitted than those carrying $-\xi$. Top right inset: Energy profile of the exchange step; E is the longitudinal kinetic energy along z and $2w$ is the exchange splitting in the magnetic materials.

$\gamma_c(k_2^2+\xi^2)+w$, where k_1 (k_2) is the z component of the wave vector in the lower (upper) subband. These expressions are correct up to first order in γ provided $|\widetilde{\gamma}\xi^2 k/w| \ll 1$ and $|\gamma\xi k^2/w| \ll 1$, where $k = k_1$ or $k = k_2$. The respective eigenvectors are written

$$\mathbf{u}_{\epsilon,1}(\xi,k_1) = \left[1 - 2\epsilon i\mu k_1^2, -\epsilon(1-2\widetilde{\mu}\xi k_1)\right]/\sqrt{2}, \quad (2)$$

$$\mathbf{u}_{\epsilon,2}(\xi,k_2) = \left[1 - 2\epsilon i\mu k_2^2, \epsilon(1+2\widetilde{\mu}\xi k_2)\right]/\sqrt{2}, \quad (3)$$

where $\mu = \gamma\xi/(2w)$ and $\widetilde{\mu} = \widetilde{\gamma}\xi/(2w)$. Note that the norm of $\mathbf{u}_{\epsilon,\ell}$ ($\ell = 1$ or 2) only involves even powers of ξ likewise the direct overlap $|\langle \mathbf{u}_{\epsilon,\ell}|\mathbf{u}_{-\epsilon,\ell}\rangle|^2$ between incoming and outgoing states, so that no $\pm\xi$ transmission asymmetry can be expected in the usual tunneling models, e.g., based on interface density of states [19–21]. The asymmetry appears in full-quantum treatments involving matching conditions at interfaces and may be correctly described by embedding methods [22].

The corresponding wave functions in regions I and II can be written in a compact form:

$$\begin{aligned}\Psi_I(z) &= \alpha\mathbf{u}_{1,2}(\xi,k_2)e^{ik_2 z} + \beta\mathbf{u}_{1,1}(\xi,k_1)e^{ik_1 z} \\ &\quad + A\mathbf{u}_{1,2}(\xi,-k_2)e^{-ik_2 z} + B\mathbf{u}_{1,1}(\xi,-k_1)e^{-ik_1 z}, \quad (4)\\ \Psi_{II}(z) &= C\mathbf{u}_{-1,1}(\xi,k_1)e^{ik_1 z} + D\mathbf{u}_{-1,2}(\xi,k_2)e^{ik_2 z},\end{aligned}$$

where the α and β (resp. A and B) amplitudes stand for incident waves (resp. reflected waves) in region I, and C and D for transmitted waves in region II. Because $\mathbf{k}_\parallel$ is conserved in the transport process, we are dealing with states with the same *longitudinal* kinetic energy E along z and a total kinetic energy $\mathcal{E} = E + \gamma_c\xi^2$. The proper matching conditions are the continuity of the wave function and of the current wave $\widehat{J}\Psi_{I,II} = (1/\hbar)(\partial\widehat{H}_{I,II}/\partial k)\Psi_{I,II}$ because $\widehat{H}_{I,II}$ contains no more than quadratic k terms [23–27] and because $\hat{\gamma}/\gamma_c$ is continuous. The average transmission coefficient $T(\xi,k_1,k_2)$ upon positive and negative incidences is related to the amplitude of the transmitted wave $C(\xi,k_1,k_2)$ calculated with the initial conditions $\alpha = 0$ and $\beta = 1$ through

$$T(\xi,k_1,k_2) = \frac{|C(\xi,k_1,k_2)|^2 + |C(-\xi,k_1,k_2)|^2}{2}, \quad (5)$$

and we define the transmission asymmetry as

$$\mathcal{A}(\xi,k_1,k_2) = \frac{|C(\xi,k_1,k_2)|^2 - |C(-\xi,k_1,k_2)|^2}{|C(\xi,k_1,k_2)|^2 + |C(-\xi,k_1,k_2)|^2}. \quad (6)$$

It can be checked that, when $\widetilde{\gamma} = 0$, $\mathcal{A}(\xi,k_1,k_2)$ vanishes if α and β are real, which is a nontrivial result. The transmission of a pure up-spin incident electron into a pure down-spin state is only possible under oblique incidence via SOI which introduces off-diagonal matrix elements. Moreover, a nonvanishing diagonal part of SOI is necessary to obtain a nonzero asymmetry although the z component of the DP field along z does not depend on the sign of $k_\parallel$ [28]. Then, from now on, we take $\widetilde{\gamma} = \gamma$. The wave vector k_1 in the lower subband has to be real so that we can define $K = k_1 > 0$. We introduce the parameter $\lambda > 0$ with $k_2 = i\lambda K$, the reduced longitudinal energy $\eta = E/w = (1-\lambda^2)/(1+\lambda^2)$, and the incidence parameter $t = \xi/K$. One obtains

$$C(\xi,K,\lambda) = \left(\frac{\gamma K^2\xi}{w}\right)\frac{[(\xi/K)(3\lambda^2-1) + 2\lambda(\lambda^2-1)]}{(\lambda-i)^2}. \quad (7)$$

From Eq. (7), it can be checked that $\mathcal{A}(\xi,k_1,k_2) = 0$ if λ would be taken as purely imaginary; the asymmetry appears when the lower-energy band carries a propagative state whereas the upper one acts as a barrier sustaining an evanescent state. Transport is then described in a two-k-channel model, a propagative channel (k_1) and an evanescent channel (k_2). One obtains

$$T(t,\eta) = \frac{\gamma^2}{\gamma_c^3} w t^2(1+\eta)^2[4\eta^2(1-\eta) + t^2(1+\eta)(2\eta-1)^2] \quad (8)$$

and

$$\mathcal{A}(t,\eta) = \frac{4t\eta\sqrt{1-\eta^2}(2\eta-1)}{4\eta^2(1-\eta) + t^2(1+\eta)(2\eta-1)^2}. \quad (9)$$

Equation (8) emphasizes the increase of $T(t,\eta)$ with t and γ. The validity range defined above can be written $|t^2(\gamma K^3/\gamma_c K^2)| \ll 1$, a condition easily fulfilled.

The analytical asymmetry $\mathcal{A}$ is plotted in Fig. 2(a) for several values of t (full lines), where the symbols refer to the 2×2 numerical calculations, showing an excellent agreement. It can be seen that the curves related to t and $t' = 1/t$ are located at almost symmetrical positions with respect to the $t = 1$ curve. They admit four zeros in the energy range considered: (i) two at the two ends of the energy step when either the propagative or the evanescent state disappears and (ii) one in the middle of the energy barrier and one for $\eta = 3/4$ which is

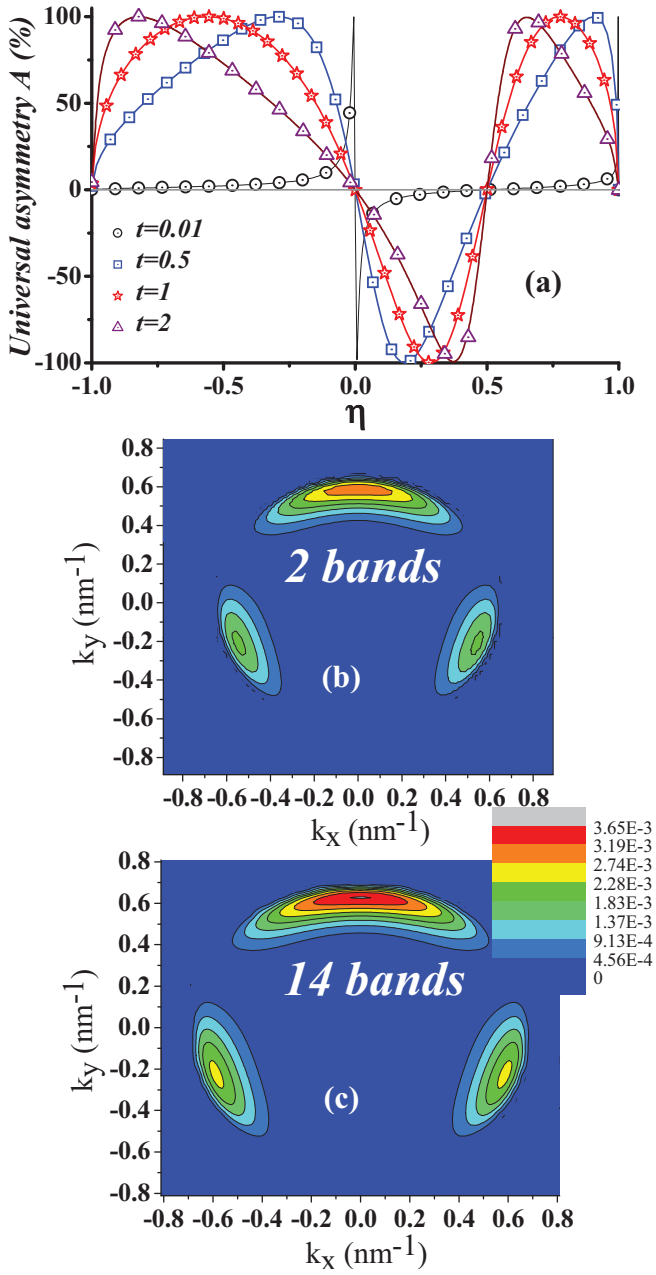

FIG. 2. (Color) (a) Universal asymmetry coefficient $\mathcal{A}$ vs reduced energy $\eta = E/w$ obtained for different values of $t = \xi/K$ [$t = 0.01$ (black; circles), $t = 0.5$ (blue; squares), $t = 1$ (red; stars), and $t = 2$ (purple; triangles)] by 2-band analytical (full line) and numerical (symbols) calculations. Two-dimensional map of the transmission coefficient T in 2×2 (b) and 14×14 (c) $\mathbf{k} \cdot \mathbf{p}$ band models for the exchange-SOI step schematized in Fig. 1; the parameters are exchange energy $2w = 0.3$ eV, total kinetic energy $\mathcal{E} = 0.08$ eV counted from the middle of the conduction step, and $\gamma = -24$ eV Å^3; band parameters of the 14-band $\mathbf{k} \cdot \mathbf{p}$ model taken from Ref. [30].

particular to Dresselhaus interaction. It is a remarkable result that $\mathcal{A}(t,\eta)$ does not depend either on the material parameters or on the sign of γ, thus conferring to $\mathcal{A}$ a universal character. Reversing the magnetization (changing w into $-w$) makes transport occur in the k_2 channel leading to a change of $\mathcal{A}(t,\eta)$ into $-\mathcal{A}(t,\eta)$ [29]. An important result is that $\mathcal{A}$ is positive when $(\mathbf{m},\boldsymbol{\xi},\mathbf{k})$ forms a direct frame and negative otherwise. Another striking feature is that an arbitrarily small perturbation is able to produce a 100% transport asymmetry, i.e., a total quenching of transmission. Figures 2(b) and 2(c) display the 2-dimensional map of the electron transmission at a given total energy in the reciprocal space calculated using both a 2×2 effective Hamiltonian [Fig. 2(b)] and a full 14×14 band $\mathbf{k} \cdot \mathbf{p}$ treatment [Fig. 2(c)] involving odd-potential coupling terms P' and Δ' [30–32]. These calculations are based on the multiband transfer matrix technique [23,24,33]. We have checked that transport asymmetry also arises for a tunnel junction where a thin tunneling barrier is inserted between the two magnetic layers. Tailoring more complicated structures which involve resonant tunneling effects allows one to obtain much higher transmission (a fraction of unity) while keeping the same magnitude for $\mathcal{A}$ [34].

We can calculate the transmitted current, $\mathbf{J}[t,\eta] = \mathbf{J}_{\xi}[\Psi_{II}(z)] + \mathbf{J}_{-\xi}[\Psi_{II}(z)]$, originating from incident waves of equal amplitude with opposite $k_{\parallel}$. To the lowest order in γ, we find

$$\mathbf{J}_{y,z}[t,\eta] = \frac{4(\gamma_c w)^{1/2}}{\hbar}(1+\eta)^{1/2} T(t,\eta)[\mathcal{A}(t,\eta)t\widehat{y} + \widehat{z}]. \quad (10)$$

Thus, the asymmetrical transmission gives rise to a transverse momentum and then to a tunneling surface current (per unit length) $j_y = J_y \times \ell_{\mathrm{mfp}}$ (ℓ_{mfp} is the electron mean-free path) which leads to an anomalous tunnel Hall effect (THE) under the steady-state regime. This effect could be experimentally investigated at a scale where the thickness of the channel collecting the current is comparable to ℓ_{mfp}, i.e., not exceeding a few nm [35]. The ratio of the (surface) transverse to the longitudinal current $j_y[t,\eta]/J_z[t,\eta] = t\mathcal{A}(t,\eta)\ell_{\mathrm{mfp}}$ then defines the THE length in the spirit of a recent work dealing with the IEE phenomenon [9,10]. To gain some numerical insight, an incident beam in region I with a given angular dispersion with respect to the z axis gives rise, after angular averaging at a fixed given energy [36], to a THE length $t\mathcal{A}\ell_{\mathrm{mfp}}$ of the order of ℓ_{mfp} for a beam deviation as large as 45° [34].

What happens for the valence bands simply described within the 6-band Luttinger $\mathbf{k} \cdot \mathbf{p}$ effective Hamiltonian [37]? The results are shown in Fig. 3; we have checked that the 14-band model provides similar data with $P' = 0$ and $\Delta' = 0$, surprisingly showing that the absence of inversion symmetry is not a key feature in the valence band. The lower curve displays the asymmetry $\mathcal{A}$ vs hole energy $\mathcal{E}$ in the case of a 3-nm-thick tunnel barrier. The energy range covers the valence spin subbands, namely, starting from the highest energy, the up-spin heavy (light) hole band $HH\uparrow$ ($LH\uparrow$), the down-spin light (heavy) hole band $LH\downarrow$ ($HH\downarrow$), and the up (down) spin split-off band $SO\uparrow(SO\downarrow)$. We refer to points (1) to (6) marked by vertical arrows in the following discussion. Here, the energy of the $HH\uparrow[HH\downarrow]$ maximum corresponds to 0.15 eV[−0.15 eV], the energy origin being taken at the top of the valence band of the nonmagnetic material, and is indicated by point (1) [(4)]. Correspondingly, one observes an almost fully negative transmission asymmetry in this energy range for predominant majority up-spin injection as far as $HH\downarrow$ does not contribute to the current. At more negative energy [$\mathcal{E} < -0.15$ eV: point (4)], a sign change of $\mathcal{A}$ occurs at the onset of $HH\downarrow$ (in the upper left inset, see the step in the transmission coefficient, which reaches almost +50%); $\mathcal{A}$ remains positive after crossing $SO\uparrow$

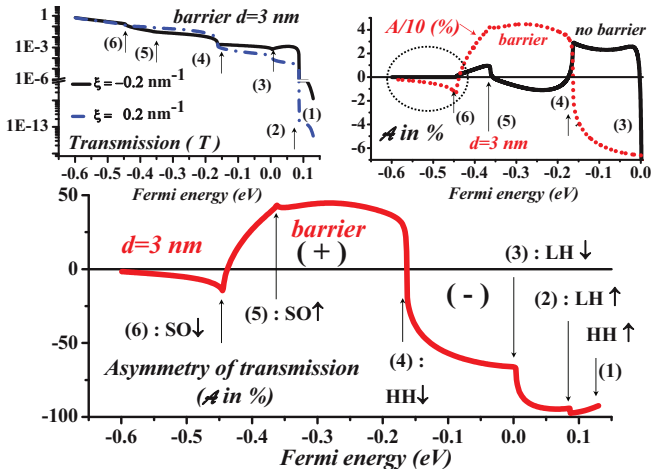

FIG. 3. (Color) Bottom: Transmission asymmetry $\mathcal{A}$ vs total energy $\mathcal{E}$ for a magnetic tunnel junction in the AP state. The parameters are $2w = 0.3$ eV, parallel wave vector $\xi = 0.2$ nm^{-1}, barrier thickness $d = 3$ nm, and barrier height 0.6 eV. The energy zero corresponds to the nonmagnetic upper-valence-band maximum. Upper left inset: Transmission T calculated in the AP state; upper right inset: asymmetry $\mathcal{A}$ without tunnel barrier ($d = 0$; black) compared to the case of the tunnel junction (dotted red).

[point (5)] before turning negative again once crossing $SO\downarrow$ [point (6)]. Note that $\mathcal{A}$ changes sign two times at characteristic energy points corresponding to a sign change of the injected particle spin. We have performed similar calculation for a simple contact ($d = 0$; right upper inset in Fig. 3, black curve). Remarkably, $\mathcal{A}$, although smaller, keeps the same trends as for the 3-nm tunnel junction, except for a change of sign, showing a subtle dependence of the exchange coupling on the barrier thickness. Without tunnel junctions, $\mathcal{A}$ abruptly disappears as soon as $SO\downarrow$ contributes to tunneling (circle region) i.e., when evanescent states disappear. In the case of tunnel junction, $\mathcal{A}$, although small, subsists in this energy range and this should be related to the evanescent character of the wave function in the barrier.

To gain physical insight in the case of the valence bands, let us start from a semiconductor toy model with conduction and valence states described by Kane's S, X, Y, and Z real cubic harmonics (no SOI) [38]. Assume that the exchange-split semiconductors are separated by a barrier involving SOI, hereafter introduced as a perturbation. Then, the relevant wave functions in the barrier are respectively associated with the wave vectors $\xi\widehat{y} \pm i\lambda K\widehat{z} = K(t\widehat{y} \pm i\lambda\widehat{z})$ to the left (+) and right (−). To second order, $\mathbf{k}\cdot\mathbf{p}$ perturbation shows that only the Y and Z valence wave functions become coupled through the conduction state, leading to two energy subsets with eigenstates $\mp i\lambda Y + tZ$ (no energy change) and $tY \pm i\lambda Z$ with an energy shift in the gap equal to $(\lambda^2 - t^2)(KP)^2/E_G$, with $P^2 = |(2\gamma_c/\hbar)\langle S|\widehat{p}_z|Z\rangle|^2$. In the AP state, $(-i\lambda Y + tZ)\uparrow$ to the left [resp. $(tY + i\lambda Z)\uparrow$] and $(i\lambda Y + tZ)\downarrow$ to the right [resp. $(tY - i\lambda Z)\downarrow$] belong to the same energy shell, resulting in efficient matching at particular incidence t. These eigenstates are carrying orbital momentum along x, namely $\langle L_x\rangle$ proportional to $-\lambda t$, whereas $\langle L_y\rangle = \langle L_z\rangle = 0$. Branching $\mathbf{L}\cdot\mathbf{S}$ SOI into the barrier lifts the energy degeneracy between states of same spin associated with $\pm t$ and affects the matching conditions so that asymmetry arises. These effects can be seen as *chirality* phenomena for scattering, analogous to magnetic circular dichroism for the optical absorption in ferromagnets. It makes understandable why the association of propagating and evanescent wave vector components may enhance spinorbitronic effects.

We have presented theoretical evidence for large interfacial scattering asymmetry of carriers vs incidence in semiconducting exchange steps and tunnel barriers. The effect appears to be robust. Direct experimental investigations can probably be performed through angle-resolved photoemission spectroscopy. After averaging over incoming states, a current perpendicular to the barrier is significantly deflected upon tunneling resulting in tunnel Hall effects and paving the way to original functionalities. Preliminary results indicate that the tunneling asymmetry in the valence band may play an important role in the analysis of tunneling anisotropy magnetoresistance data [34].

The authors express their gratitude to G. Fishman, J.-M. Jancu, and T. Wade, for valuable advice. H. J. thanks S. Blügel for stimulating discussions. T.H.D. acknowledges Idex Paris-Saclay and Triangle de la Physique for funding. T.L.H.N. is supported by Vietnam National Foundation for Science and Technology Development (NAFOSTED) under Grant No. 103.01-2013.25.

[1] L. Liu, O. J. Lee, T. J. Gudmundsen, D. C. Ralph, and R. A. Buhrman, Current-induced switching of perpendicularly magnetized magnetic layers using spin torque from the spin Hall effect, Phys. Rev. Lett. **109**, 096602 (2012).

[2] I. M. Miron, G. Gaudin, S. Auffret, B. Rodmacq, A. Schuhl, S. Pizzini, J. Vogel, and P. Gambardella, Current-driven spin torque induced by the Rashba effect in a ferromagnetic metal layer, Nat. Mater. **9**, 230 (2010).

[3] K. Garello, I. M. Miron, C. O. Avci, F. Freimuth, Y. Mokrousov, S. Blügel, S. Auffret, O. Boulle, G. Gaudin, and P. Gambardella, Symmetry and magnitude of spin–orbit torques in ferromagnetic heterostructures, Nat. Nano. **8**, 587 (2013).

[4] J.-C. Rojas-Sánchez, N. Reyren, P. Laczkowski, W. Savero, J.-P. Attané, C. Deranlot, M. Jamet, J.-M. George, L. Vila, and H. Jaffrès, Spin pumping and inverse spin Hall effect in platinum: The essential role of spin-memory loss at metallic interfaces, Phys. Rev. Lett. **112**, 106602 (2014).

[5] Y. A. Bychkov and E. I. Rashba, Properties of a 2D electron gas with lifted spectral degeneracy, Pis'ma v ZhETF **39**, 66 (1984) [JETP Lett. **39**, 78 (1984)].

[6] G. Bihlmayer, Y. M. Koroteev, P. M. Echenique, E. V. Chulkov, and S. Blügel, The Rashba effect at metallic interface, Surf. Sci. **600**, 3888 (2006).

[7] O. Krupin, G. Bihlmayer, K. M. Dobrich, J. E. Prieto, K. Starke, S. Gorovikov, S. Blügel, S. Kevan, and G. Kaindl, Rashba effect at the surfaces of rare-earth metals and their monoxides, New J. Phys. **11**, 013035 (2009).

[8] P. Gambardella and I. M. Miron, Current-induced spin–orbit torques, Philos. Trans. R. Soc. A **369**, 3175 (2011).

[9] J. C. Rojas Sánchez, L. Vila, G. Desfonds, S. Gambarelli, J. P. Attané, J. M. De Teresa, C. Magén, and A. Fert, Spin-to-charge conversion using Rashba coupling at the interface between non-magnetic materials, Nat. Commun. **4**, 2944 (2013).

[10] S. Sangiao, J. M. De Teresa, L. Morellon, I. Lucas, M. C. Martinez-Velarte, and M. Viret, Control of the spin to charge conversion using the inverse Rashba-Edelstein effect, Appl. Phys. Lett. **106**, 172403 (2015).

[11] P. S. Alekseev, Tunneling Hall effect, JETP Lett. **92**, 788 (2010).

[12] V. I. Perel', S. A. Tarasenko, I. N. Yassievich, S. D. Ganichev, V. V. Bel'kov, and W. Prettl, Spin-dependent tunneling through a symmetric semiconductor barrier, Phys. Rev. B **67**, 201304(R) (2003).

[13] S. A. Tarasenko, V. I. Perel', and I. N. Yassievich, In-Plane electric current is induced by tunneling of spin-polarized carriers, Phys. Rev. Lett. **93**, 056601 (2004).

[14] P. C. van Son, H. van Kempen, and P. Wyder, Boundary resistance of the ferromagnetic-nonferromagnetic metal interface, Phys. Rev. Lett. **58**, 2271 (1987).

[15] T. Valet and A. Fert, Theory of the perpendicular magnetoresistance in magnetic multilayers, Phys. Rev. B **48**, 7099 (1993).

[16] An asymmetry also occurs when a single magnetic electrode is considered (region *I*) and a paramagnet in region *II*, or when two different ferromagnets are considered both in AP and PA configurations. This would lead to four different resistance states. On the other hand, the case of Rashba interactions via an external electric field leading to a curvature of the band profile is excluded from this discussion. This can lead to asymmetry of scattering in the parallel case.

[17] G. Dresselhaus, Spin-orbit coupling effects in zinc blende structures, Phys. Rev. **100**, 580 (1955).

[18] M. I. D'yakonov and V. I. Perel', Spin orientation of electrons associated with the interband absorption of light in semiconductors, Zh. Eksp. Teor. Fiz. **60**, 1954 (1971) [Sov. Phys. JETP **33**, 1053 (1971)].

[19] J. Bardeen, Tunnelling from a many-particle point of view, Phys. Rev. Lett. **6**, 57 (1961).

[20] M. Jullière, Tunneling between ferromagnetic films, Phys. Lett. A **54**, 225 (1975).

[21] J. C. Slonczewski, Conductance and exchange coupling of two ferromagnets separated by a tunneling barrier, Phys. Rev. B **39**, 6995 (1989).

[22] D. Wortmann, H. Ishida, and S. Blügel, Embedded Green-function approach to the ballistic electron transport through an interface, Phys. Rev. B **66**, 075113 (2002).

[23] A. G. Petukhov, A. N. Chantis, and D. O. Demchenko, Resonant enhancement of tunneling magnetoresistance in double-barrier magnetic heterostructures, Phys. Rev. Lett. **89**, 107205 (2002).

[24] M. Elsen, H. Jaffrès, R. Mattana, M. Tran, J.-M. George, A. Miard, and A. Lemaître, Exchange-mediated anisotropy of (Ga,Mn)As valence-band probed by resonant tunneling spectroscopy, Phys. Rev. Lett. **99**, 127203 (2007).

[25] T. L. Hoai Nguyen, H.-J. Drouhin, J.-E. Wegrowe, and G. Fishman, Spin rotation, spin filtering, and spin transfer in directional tunneling through barriers in noncentrosymmetric semiconductors, Phys. Rev. B **79**, 165204 (2009).

[26] H.-J. Drouhin, G. Fishman, and J. E. Wegrowe, Spin currents in semiconductors: Redefinition and counterexample, Phys. Rev. B **83**, 113307 (2011).

[27] F. Bottegoni, H.-J. Drouhin, G. Fishman, and J.-E. Wegrowe, Probability- and spin-current operators for effective Hamiltonians, Phys. Rev. B **85**, 235313 (2012).

[28] This fact immediately proves that the effect we describe does not exist in the spin-filter asymmetry considered in Refs. [11,12], where the DP spin-orbit Hamiltonian reduces to $\gamma(\widehat{\sigma}_x k_x - \widehat{\sigma}_y k_y)\partial^2/\partial z^2$, the term proportional to $\widehat{\sigma}_z$ being neglected.

[29] Transport now involves the $D(\xi,k_1,k_2)$ coefficient which can be deduced from $C(\xi,k_1,k_2)$ by interchanging k_1 and k_2 as well as ξ to $-\xi$, resulting in the change of $\mathcal{A}(t,\eta)$ into $\mathcal{A}(-t,\eta) = -\mathcal{A}(t,\eta)$ (this can also be simply checked by symmetry considerations).

[30] J.-M. Jancu, R. Scholz, E. A. de Andrada e Silva, and G. C. La Rocca, Atomistic spin-orbit coupling and k. p parameters in III-V semiconductors, Phys. Rev. B **72**, 193201 (2005).

[31] M. Cardona, N. E. Christensen, and G. Fasol, Relativistic band structure and spin-orbit splitting of zinc-blende-type semiconductors, Phys. Rev. B **38**, 1806 (1988).

[32] P. Pfeffer and W. Zawadzki, Conduction electrons in GaAs: Five-level k.p theory and polaron effects, Phys. Rev. B **41**, 1561 (1990).

[33] The boundary conditions at interfaces are (i) the continuity of the components of the envelope function, $\psi_n^+ + \sum_{\bar{n}} r_{n,\bar{n}}\psi_{\bar{n}}^- = \sum_{n'} t_{n,n'}\psi_{n'}^+$, where (+) [(−)] refer to wave functions propagating to the right (to the left), and $t_{n,n'}(r_{n,\bar{n}})$ is the amplitude of the transmitted (reflected) wave in band $n'(\bar{n})$ for a normalized incident wave in band n; (ii) the continuity of the components of the current wave, $\widehat{J}\psi_n^+ + \sum_{\bar{n}} r_{n,\bar{n}}\widehat{J}\psi_{\bar{n}}^- = \sum_{n'} t_{n,n'}\widehat{J}\psi_{n'}^+$. With conservation of $k_\parallel$, the multiband transmission is written $T_{n,n'}(\xi) = [t_{n,n'}]^* t_{n,n'}\langle\psi_{n'}|\widehat{J}|\psi_{n'}\rangle/\langle\psi_n|\widehat{J}|\psi_n\rangle$.

[34] See Supplemental Material at http://link.aps.org/supplemental/10.1103/PhysRevB.92.060403 for a numerical estimation.

[35] It can be checked that the THE voltage is of the order of $(\rho/\delta)L\ell_{\mathrm{mfp}}t\mathcal{A}(t,\eta)J_z$, where L is the lateral size of the junction, ρ the resistivity, and δ the thickness of the collecting channel.

[36] The relationship $\eta = (-t^2 + \mathcal{E}/w)/(1+t^2)$ relates η to the reduced total energy $\mathcal{E}/w$ and the angular averaging is performed with $d\theta = dt/(1+t^2)$.

[37] J. M. Luttinger, Quantum theory of cyclotron resonance in semiconductors: General theory, Phys. Rev. **102**, 1030 (1956).

[38] E. O. Kane, Band structure of indium antimonide, J. Phys. Chem. Solids **1**, 249 (1957).